Energy & Buildings 202 (2019) 109378

Contents lists available at ScienceDirect

Energy & Buildings

journal homepage: www.elsevier.com/locate/enbuild

# Towards climate robust buildings: An innovative method for designing buildings with robust energy performance under climate change

Amin Moazami[a,*], Salvatore Carlucci[a], Vahid M. Nik[b,c,d], Stig Geving[a]

[a] NTNU Norwegian University of Science and Technology, Department of Civil and Environmental Engineering, 7491, Trondheim, Norway
[b] Division of Building Physics, Department of Building and Environmental Technology, Lund University, 223 63, Lund, Sweden
[c] Division of Building Technology, Department of Civil and Environmental Engineering, Chalmers University of Technology, 412 58, Gothenburg, Sweden
[d] Institute for Future Environments, Queensland University of Technology, Garden Point Campus, 2 George Street, Brisbane, QLD, 4000, Australia

ARTICLE INFO

*Article history:*
Received 23 April 2019
Revised 9 August 2019
Accepted 18 August 2019
Available online 19 August 2019

*Keywords:*
Robust design optimization
Robust design
Climate change
Building performance simulation
Primary energy
Climate uncertainty
Extreme conditions
Simulation-based optimization

ABSTRACT

Neglecting extremes and designing buildings for the past or most likely weather conditions is not the best approach for the future. Robust design techniques can, however, be a viable option for tackling future challenges. The concept of robust design was first introduced by Taguchi in the 1940s. The result of the design process is a product that is insensitive to the effect of given sources of variability, even though the sources themselves are not eliminated. A robust design optimization (RDO) method is for the first time proposed in this paper, for supporting architects and engineers in the design of buildings with robust energy performance under climate change and extreme conditions. The simplicity and the low computational demand of the process underlies the feasibility and applicability of this method, which can be used at any stage of the design process. The results show that the performance of the optimum solution not only has a 81.5% lower variation (less sensitivity to climate uncertainty) but at the same time has a 14.4% lower mean energy use value compared with a solution that is compliant with a recent construction standard (ASHRAE 90.1-2016). Less sensitivity to climate uncertainty means greater robustness to climate change whilst maintaining high performance.



## 1. Introduction

The focus of building designers, architects and engineers in the design of buildings has, in recent years, been orientated towards minimizing the energy use of buildings or achieving a net zero energy balance (ZEB) at the building or neighborhood scale. Building performance simulation (BPS) has been a powerful tool helping to reach solutions for better energy efficiency. Studies have, however, shown that more optimal solutions can be achieved using automated optimization techniques [1]. Nguyen et al. [2] reviewed simulation-based optimization methods and concluded that a further reduction of 20- 30% can be achieved in building energy consumption using automated optimization. Advancements in computational science and the desire to achieve higher levels of energy optimality mean the use of simulation-based optimization techniques is on the rise in the building sector [3]. These techniques allow designers to systematically explore a wider design space and to so find better solutions. This is made possible by coupling an automated mathematical optimization tool with a BPS program. During the building simulation process, many different design options are evaluated to obtain the optimum for a set of objectives (e.g. zero energy balance) [4]. These promising technologies therefore help to achieve high performance design solutions. Buildings constructed based on these design solutions are, however, usually very sensitive to changes in operational conditions. The performance gap between expected performance and actual level of performance has been discussed and demonstrated in the literature [5–7]. There are a number of factors that influence the discrepancy between the designed and constructed performance of buildings. The sources of this discrepancy can be categorized into three types: epistemic uncertainties, aleatory uncertainties and errors. Epistemic uncertainty is defined as "*a potential deficiency that is due to a lack of knowledge.*" [8]. Examples of epistemic uncertainties are the simplifications and numerical approximations of physical processes considered in numerical models of BPS tools [9]. An error is defined as "*the discrepancy between a computed,*

* Corresponding author.
*E-mail addresses:* amin.moazami@ntnu.no (A. Moazami), salvatore.carlucci@ntnu.no (S. Carlucci), vahid.nik@byggtek.lth.se, vahid.nik@chalmers.se, vahid.nik@qut.edu.au (V.M. Nik), stig.geving@ntnu.no (S. Geving).

https://doi.org/10.1016/j.enbuild.2019.109378

**Nomenclature and acronyms**

| | |
|---|---|
| AR | Augmented Reality |
| BIM | Building Information Modelling |
| BPS | Building Performance Simulation |
| CDD | Cooling Degree Days |
| ECY | Extreme Cold Year |
| EWY | Extreme Warm Year |
| GCM | General Circulation Model |
| HDD | Heating Degree Days |
| MOGA-II | Multi-Objective Genetic Algorithm |
| MSD | Mean Squared Deviation |
| NSGA-II | Fast Non-dominated Sorting Genetic Algorithm |
| PE | Primary Energy |
| RCM | Regional Climate Model |
| RDO | Robust Design Optimization |
| TMY | Typical Meteorological Year |
| ZEB | Zero Energy Balance |

*observed or measured value or condition and the true, specified or theoretically correct value or condition*" [10]. Examples of source of errors are discrepancies between constructed and simulated buildings due to human errors during construction and the use of poorer quality construction materials than designed [11]. The third type is aleatory uncertainty which is the "*uncertainty that is said to arise due to the inherently random or variable nature of a quantity, or the (usually unknown) system underlying it.*" [9]. Examples of discrepancies due to aleatory uncertainties are the influence of occupants' behavior and/or climate conditions on the performance of buildings. The first two sources of discrepancy, epistemic uncertainty and errors, are reducible. Aleatory uncertainty is, however, irreducible and cannot be eliminated due to its inherent randomness and natural variability [12]. *Epistemic uncertainties* in building modeling can be reduced by improving numerical models, calibrating using additional experimental observations, and providing better information [13]. E*rrors* can be minimized by the use of technological advancements such as Building Information Modelling (BIM) [14] and Augmented Reality (AR) [15], and offsite or prefabricated construction technologies [16]. Aleatory uncertainties cannot be eliminated and the common approach to dealing with this type of uncertainty in BPS is to consider the most likely scenario. For example, occupants are normally simulated using a fixed schedule [17] as the most probable occupancy scenario. Typical meteorological year (TMY) weather files is another example of accounting for the most likely conditions [18]. This approach causes the final solution to be sensitive to variations beyond the most likely conditions, which may result in malfunctioning during adverse real life conditions. Kalkman [19] showed that there can be a difference between energy use in identically constructed buildings of up to17 times bigger due to the influence of occupants. Rastogi [9] thoroughly studied the sensitivity of building performance to climate. The best way to deal with these uncertainties is to evaluate and design buildings under presence of them. Designing under the presence of aleatory uncertainties is not a new concept and has been discussed in other fields in the industry for a long time. It has, however, not yet been applied to building design. The idea of this concept is that this source is presented as noise during the design phase instead of being eliminated. The goal therefore is to achieve a design solution with a performance that is least sensitive to the presence of noise. This process is called "robust design" and was introduced by Taguchi in the 1940s [20].

The aim of this work is to use the power of simulation-based optimization technology to discover new areas of design space, and to couple this to the experience of robust design from other industrial fields, to so achieve building designs with a robust energy performance under climate uncertainties. A robust design problem can also be formulated as an optimization problem. The concept of adding robust design to conventional optimization is called robust design optimization (RDO). The idea is to achieve minimum performance variability under the presence of uncertainty. These concepts have been widely practiced and developed in design areas ranging from car manufacturing [21] and electronics [22] to medicine [23] and chemical productions [24]. An RDO technique for the design of buildings with robust energy performance under typical and extreme conditions is proposed in this study for the first time. The main focus is to introduce a process that is relatively simple and can be used by architects and engineers from the early stage of design. The outcome of this process is a design with an energy performance that is least sensitive to climate variations and an energy use that is also minimum, i.e. energy-robust and energy-efficient under climate change.

Climate change means that it is no longer possible to design buildings based only on TMYs [25]. Climate conditions have changed and are going to continue to change, giving in the near future more frequent and intense extreme conditions [26]. A system that has been designed to meet a required performance under typical or most likely conditions can be challenged up to its failing point under atypical or extreme conditions [27]. Examples are black outs or regional grid failures during heat waves. One of the main reasons for this is the high sensitivity of buildings to the perturbation of external conditions, this causing performance to vary significantly if the conditions fall outside the typical range. For example, electricity demand that soars during heat waves is due to buildings that are not designed for such conditions. Energy system failure may leave thousands of houses with no means of cooling and puts the lives of vulnerable people at risk in overheated buildings, as happened during the 1995 Chicago heat wave [28], the 2003 Europe heat wave [29] and 2006 heat wave in New York City [30]. Heat waves are good examples of how underestimation during design can easily become very costly. Buildings of today need to be designed to not only perform optimally under typical conditions, but also show minimum variation under atypical conditions. One of the main challenges to achieving this target is considering climate uncertainty in the optimization process. Climate uncertainty and challenges in considering this in a simulation-based optimization process are discussed in Section 2.2. The concept of robust design and its implication in the built environment is described briefly in the following section. In Section 3, the proposed RDO methodology for robust energy performance under climate change is described in detail. An approach to test the effectiveness of the method is presented in Section 4, where the solutions provided by the RDO method are tested under 74 climate scenarios. The results and conclusions are provided in Section 5 and 6.

## 2. Background and concepts

### 2.1. Concept of robust design optimization and its implication in built environment

Robust design has, since being introduced, been adopted in a wide range of industries. Taguchi defined robustness as "the state where the technology, product, or process performance is minimally sensitive to factors causing variability (either in the manufacturing or user's environment) and aging at the lowest unit manufacturing cost" [31]. In other words, "a product or process is said to be robust when it is insensitive to the effect of source of variability, even though the sources themselves have not been eliminated" [32]. Further definitions of robustness from system engineering and product design are: insensitivity to anticipated risks [33], a measure of variation in performance [34], insensitivity to

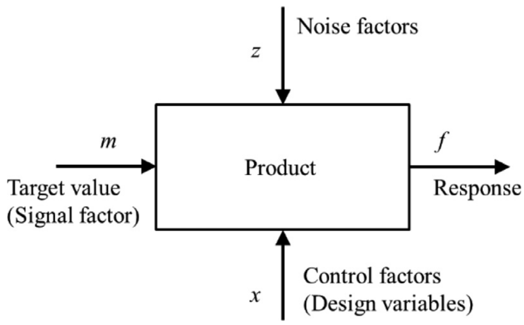


**Fig. 1.** Block diagram of a product: P diagram.

unforeseeable changes in the operating environment [35], insensitivity to both expected and unexpected variations [36], the ability of a system to continue to operate correctly across a wide range of operational conditions [37], the ability of a system to absorb change [38], the potential for system success under varying future circumstances or scenarios [39], and the ability of a system – as built/designed – to do its basic job in uncertain or changing environments [40].

Robust design of a product involves the factors defined below [41]:

- *Control factors (or Design variables)* are variables that have to be specified by the designer
- *Noise factors* are uncertain parameters that the designer cannot control (only the statistical characteristics of noise factors that are expected in production or in the actual use of the product can be known or specified)
- *Target value (Signal factor)* is set by regulations or the user of the product to express the desired value of the response of the product
- *Response* is the output of the product in the presence of noise

One application of robust design is in car manufacturing and specifically in car packaging design. The target is to achieve high car spatial and ergonomic efficiency. For example, in a study [21] of an ergonomic robust design of car packaging, the *seat cushion angle, steering-wheel-to-BOF (ball of foot) distance,* etc. were used as control factors, the *anthropometric variability* was used as a noise factor and the response was occupant *comfort loss*. The aim of a robust design was to set optimal control factors in which the variation of the response from the target value is minimum under the presence of noise factors. A block diagram representation of a product [41] is shown in Fig. 1, to explain the robust design procedure.

A robust design problem is a multi-objective optimization problem. The objectives are to reduce the variation of the response as the mean is shifted to a target value (Fig. 2).

Taguchi, based on this process, developed the signal-to-noise ratio (S/N). This is a key metric that is used to perform the first step of the optimization process. S/N is maximized in this step, which is equivalent to minimizing the sensitivity of the response to noise factors [32].

$$S/N = 10log_{10}\left[{}^{\mu^2}/_{\sigma^2}\right] \quad (1)$$

S/N is proportional to the base 10 logarithm of the ratio between the square of the signal factors ($\mu$) and the square of the noise factors ($\sigma$). Adding a logarithm to the metric was proposed by Taguchi and converts the S/N ratio into *decibels* (*dB*) [32]. Taguchi stated that a metric for robust design should have four properties [32]:

1. *The metric should reflect the variability in the response.*

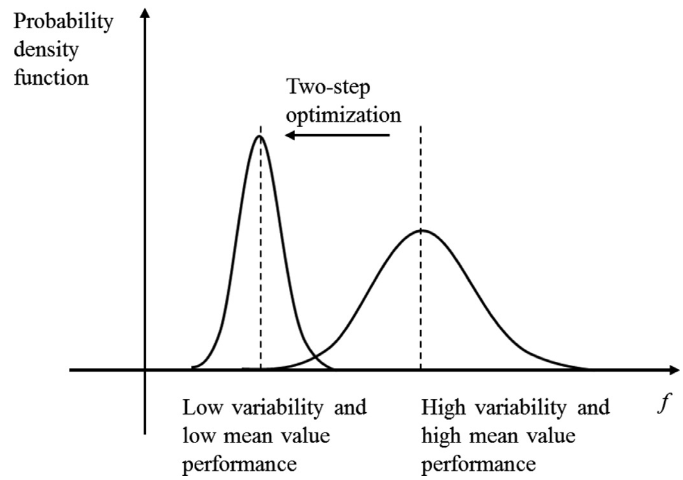


**Fig. 2.** Robust design applied to buildings performance where the smaller mean and variation of response f is desired.

2. *The metric should be independent of adjustment of the mean.*
3. *The metric should measure relative quality.*
4. *The metric should not induce unnecessary complications, such as control factors interactions.*

A good S/N metric has all of the above properties. These properties are further discussed for the S/N metric developed for this study in Section 3.4.

Robust design is a general concept that is applicable to all design procedures that take uncertainty into account. The aim is to minimize the sensitivity of a product's performance to the presence of uncertainties in real world conditions. This concept can be transferred from industrial products to buildings simply by considering the target value to be any desired performance indicator (e.g., the indoor thermal comfort condition, the indoor daylight performance or the maximum delivered energy) and the noise factor to be any variable that causes deviations in the performance of a building during operation. The concept of robustness has been discussed in the building engineering literature in terms of a variety of uncertainty sources. For example [42,43] consider the energy robustness of an office building to energy related occupant behavior. They conceptualized robustness as a minimum variation in energy use irrespective of varying occupant behavior. Leyten and Kurvers [44] studied the indoor climate robustness of an office building and state that robustness is "*the measure by which the indoor environment of a building lives up to its design purpose when it is used by occupants in a real life situation*". Palme et al. [45,46] proposed a concept for robustness of energy performance in buildings and related it to the ability of a building to mitigate the unpredictable variations induced by occupants or by external factors. Chinazzo et al. [47] assessed the robustness of energy performance to the uncertainties in weather files, and Hoes et al. [48] considered the sensitivity of several performance indicators to the effect of user behavior. They investigated several design cases to find the most robust (the least sensitive) case to user behavior. [49] investigated the robustness of energy use for lighting in the presence of occupant behavior uncertainty. Kotireddy et al. [50] developed a methodology based on scenario analysis to assess the performance robustness of low-energy buildings. These studies demonstrate that the concept of robustness in buildings has different interpretations and has not converged to a concise approach in this field of research.

Table 1 gives a non-exhaustive list of the built environment's terms classified according to the factors represented in the P diagram.

**Table 1**
Built environment's examples classified according to the factors of the P diagram.

| Product | Noise factors | Control factors (Design variables) | Responses |
|---|---|---|---|
| Building scale:<br>• components<br>• systems<br>• units/apartments<br>Urban scale:<br>• Building /Facility<br>• Neighborhood<br>• City<br>• Region | Climate conditions:<br>• Changes in long-term and short-term patterns of climate<br>Occupant behavior:<br>• Operation of appliances<br>• Manipulation of building control settings<br>• Windows operation<br>• Door operation<br>• Vent operation<br>• Use of domestic hot water | Envelope Thermal properties:<br>• Insulation thickness<br>• U-value of glazing<br>• G-value of glazing<br>Building Geometry:<br>• Air volume<br>• Window-to-wall ratio<br>• Net floor area<br>Control settings:<br>• Maximum solar irradiance to draw down solar shading devices<br>• Set point temperature to open windows for enabling natural ventilation<br>• Heating set point temperature<br>• Cooling set point temperature | • Energy use<br>• Thermal discomfort<br>• $CO_2$ concentration<br>• Visual discomfort (glare)<br>• Noise level |

Robust design process was, due to the high costs of experimental tests and the limited computational power for running simulations, originally formulated in a way that allowed the process to be performed at minimum cost and resource usage. Taguchi used an *orthogonal array* approach. This is a method for setting experiments with only a fraction of the full combinations [32]. The availability of better numerical models and high computational power means that this concept was later introduced into a simulation-based optimization process, and is referred to as robust design optimization (RDO) [51]. RDO, in other words, adds the concept of robust design to conventional optimization [52,53]. The deterministic approach used in conventional optimization does not consider the impact of unavoidable uncertainties (noise factors) associated with input design variables in a real engineering environment. This results in optimum solutions that have a sensitive performance measure and can vary significantly with the distribution of noise factors. The design problems of building engineering can also be formulated as RDO problems, the objective being to achieve a performance measure (e.g. energy) with minimum sensitivity to a noise factor (e.g. climate).

A number of design variables of an office building are optimized in this study to achieve a minimum variation of their energy performance under the disturbance of mutable climate variables. In this case, the noise factor is climate change and the objectives of the RDO scheme are to minimize mean energy performance and at the same time minimize energy performance variability under climate change. Inspired by the work of Taguchi, two metrics (two objective functions) were developed for an optimization process that results in solutions with minimum variation in energy performance of a building under the presence of climate uncertainty. The first objective is an S/N ratio metric customized for the purpose of this study and that fulfills the four properties described earlier. The second objective focuses on minimizing energy use. These metrics are introduced in Section 3.4.

The first challenge in the intended RDO process is introducing climate change as a noise factor into the optimization problem. The following section is dedicated to climate uncertainty and challenges considering this in simulation-based optimization.

### *2.2. Climate uncertainty and simulation-based optimization*

Detailed weather data with a daily or hourly resolution is required to properly describe (through simulation) the dynamic energy behavior of a building [54]. Weather data defines the external boundary conditions for BPS. Current practice in BPS is to use typical meteorological year (TMY) weather files. These represent the most likely climate conditions based on historical recorded data [18]. TMYs are one-year weather files of typical conditions for a 30-year period of measured data for a given location. One of the main disadvantages of this method is its averaging nature: the generation of a typical weather year neglects extreme weather conditions. Today's technology, climate model data such as General Circulation Models (GCMs) and Regional Climate Models (RCMs) can provide information on possible future climate conditions. These models are able to generate years of future climate data based on different climate scenarios [55] for most locations on earth. Future climate data must, however, be converted into a suitable format for use in BPS. Moazami et al. [56] investigated the techniques available to convert this data into suitable resolutions for BPS and design purposes. It is theoretically possible today, to take into account climate uncertainty, to run a design under 100 of years of consistent climate data of past recorded data and future possible climate scenarios. The availability of this data makes it possible to study the sensitivity of a design or to look for design alternatives that demonstrate minimum sensitivity to climate conditions. This however means that hundreds of simulation runs must be performed at each optimization step to calculate the RDO objectives. The optimization scheme may therefore become infeasible due to high computational cost. The following example helps us gain a feeling of the time and the computation resources required to consider all possible scenarios and minimize mean and variation of energy performance under these scenarios. Let us, for example, consider 30 years of future climate data with an ensemble of 4 generated scenarios (two GCM-RCMs and two emission scenario). 30 years of historical data are also available. These provide 150 years of climate data. Each optimization process step will therefore contain 150 annual simulations. In other words, 150,000 simulation runs are required for an optimization process of 1000 evaluations. Each simulation takes 1 min and four parallel simulations can be run. The optimization process will therefore take around 26 days. The required time-scale is therefore not feasible in building design practice.

Work by Nik [57] proposed a method to synthesize a set of representative weather data sets, this including one typical year and two extreme cold and warm years. These are the Typical Downscaled Year (TDY), Extreme Cold Year (ECY) and Extreme Warm

Year (EWY). This can solve the problem of high numbers of simulations and of the exclusion of extreme conditions. The method has the advantage of substantially decreasing the number of simulations, while taking extreme conditions and future climate uncertainties into account. The method for generating TDY, ECY and EWY is explained in detail in [57]. In short, the method is based on Finkelstein–Schafer (FS) statistics [18] - picking the months with a cumulative distribution temperature most like the whole data sets for typical months and constructing TDY based on these. ECY and EWY pick the months with the largest differences for the extreme cold and warm cases. The method and its usefulness have been verified in different applications [56–58]. The method for synthesizing representative weather data sets was developed further to track all possible extremes at each time step for any desired climate variable. This required the typical and extreme values of a climate variable to be picked according to the hourly (instead of monthly) distribution at each time step (hour) for all years and climate scenarios. This resulted in three time-series (length of 8760 h), each containing the most typical, the lowest and the highest values at each time step. These data sets are only generated for calculation purposes and cannot be considered to be weather data, as they do not reflect the natural variations of the climate system (unlike TDY, ECY and EWY which are arranged based on monthly distributions and reflect natural variations). Nevertheless, each hourly value is a possible future condition that may challenge the designs.

The above approach allows climate change to be applied in simulations as a noise factor using only three weather files (three years of climate data). This means that the number of simulation runs for this example is reduced to 3000 (1000 evaluation × 3 simulation runs using TDY, ECY and EWY weather files), the optimization process therefore requiring 12.5 h.

This study used weather files generated for the city of Geneva. Geneva was chosen due to the wealth of available data and the possibility of representing both cold winters and warm summers. The set of the representative weather files was synthesized in a previous study [56].

## 3. Simulation-based optimization method for design of energy-efficient buildings with robust energy performance

We, in this paper, specifically refer to a multi-objective RDO that identifies a set of optimal building design solutions for achieving robust energy performance and high efficiency. The set of design solutions give buildings high energy-efficiency and low performance-variability when a noise factor is present. It furthermore implies low energy use and a minimum sensitivity to disturbances. This specific robust design optimization problem can be formulated as:

$$\min_{x \in \mathbb{R}^n} \{f_1(\boldsymbol{x}, \boldsymbol{u}_i), f_2(\boldsymbol{x}, \boldsymbol{u}_i)\} \tag{2}$$

$$g_i(\boldsymbol{x}, \boldsymbol{u}_i) \leq 0 \ \forall \boldsymbol{u}_i \in \mathcal{U}_i, \ \ i = 1, \ldots, r \tag{3}$$

$$x_L \leq x \leq x_U \tag{4}$$

where $\boldsymbol{x}$ is the vector of design variables, $f_1(\boldsymbol{x}, \boldsymbol{u}_i)$ and $f_2(\boldsymbol{x}, \boldsymbol{u}_i)$ are the objective functions, and $g_i(\boldsymbol{x}, \boldsymbol{u}_i)$ are inequality constraints that are subject to the uncertainty parameters that can take any arbitrary value in the *uncertainty domain* $\mathcal{U}_i \subseteq \mathbb{R}^m$. Using this formalism, the goal of this robust design optimization problem is to find a *set* $X(\mathcal{U}_i)$ (i.e. the set of the minimum-cost building variants) from all the available building variants which is feasible where all noises factors $\boldsymbol{u}_i \in \mathcal{U}_i$ are taken into consideration.

$$X(\mathcal{U}_i) = \{x | g_i(\boldsymbol{x}, \boldsymbol{u}_i) \leq 0 \ \forall \boldsymbol{u}_i \in \mathcal{U}_i, \ \ i = 1, \ldots, r\}. \tag{5}$$

The design effect of these two objectives is, as shown in Fig. 2, a narrow distribution of primary energy with a mean value close to the target value (ideally zero). Optimizing $f_1(\boldsymbol{x}, \boldsymbol{u}_i)$ will minimize the sensitivity of performance to noise and is a measure of robustness. Optimizing $f_2(\boldsymbol{x}, \boldsymbol{u}_i)$ will minimize primary energy use and is a measure of energy-efficiency. These effects are visualized in Fig. 3.

### 3.1. Formulating the objective functions

The focus of this study is, as mentioned previously, to achieve robustness to climate uncertainty. The distribution of energy performance (e.g. Fig. 3) is therefore only a result of variations in climate. The method suggested by Nik [57] was adopted to use climate as a source of performance variability and uses one typical and two extreme weather files (to be called the triple method hereafter). It is described in Section 2.2. The range of climate scenarios is, in this method, summarized into three weather files: TDY, EWY and ECY. The TDY file represents the most likely climate evolution and EWY and ECY are the extreme warm and cold climate evolutions. $PE_{TDY,\,i}$, $PE_{ECY,\,i}$ and $PE_{EWY,\,i}$ are the primary energy use (PE) calculated for the time-step $i$ using the TDY, EWY and ECY weather files.

The four properties described in Section 2.1 were considered in the development of a custom S/N ratio for this study. The first property is that a metric is defined that *reflects the variability in the response*. The mean squared deviation (MSD) is therefore calculated, which is the average squared differences for the $PE_{ECY,\,i}$ and $PE_{EWY,\,i}$ values with $PE_{TDY,\,i}$ as reference values. Using $PE_{TDY,\,i}$ as reference values allows this function to be used to measure how far the values of $PE_{ECY,\,i}$ and $PE_{EWY,\,i}$ are from the reference values. This can then be used as a measure of variability. The second property requires the metric to be *independent of adjustment of the mean*. A second objective function was therefore introduced. The calculated value of $PE_{TDY,\,i}$ is, in this objective, separately minimized, which makes the first objective independent of adjustment of $PE_{TDY,\,i}$. The third property is that *the metric should measure relative quality*. The S/N is calculated as relative change of $PE_{TDY,\,i}$ squared to MSD. The final step, proposed by Taguchi, was adding a logarithm to the metric, so converting the S/N ratio into *decibels* (dB). This transforms the multiplicative changes in the metrics to additive changes, which helps reduce the effect of interactions between the design variables [32]. It furthermore means that the influence of each design variable is independent of the effects of the other design variables, so meeting the condition of the fourth property. This metric is formulated as objective function no.1 and is descried below. Minimizing the first objective also minimizes the difference between energy performance under extreme and typical conditions, which also minimizes the sensitivity of the response to changing climate. The second objective at the same time minimizes the annual primary energy $PE_{TDY,\,i}$, which is the annual total primary energy required by the building under average conditions (TDY). These objectives are formulated as below:

**Objective function n.1**: the purpose of $f_1(\boldsymbol{x}, \boldsymbol{u}_i)$ is to squeeze the energy performance calculated using EWY and ECY towards the performance calculated using TDY. MSD is therefore here defined as:

$$MSD = \frac{1}{2\boldsymbol{p}} \sum_{\boldsymbol{i}=1}^{\boldsymbol{p}} \left[ \left( PE_{ECY_{(\boldsymbol{u}_1),\boldsymbol{i}}} - PE_{TDY_{(\boldsymbol{u}_1),\boldsymbol{i}}} \right)^2 + \left( PE_{EWY_{(\boldsymbol{u}_1),\boldsymbol{i}}} - PE_{TDY_{(\boldsymbol{u}_1),\boldsymbol{i}}} \right)^2 \right] \tag{6}$$

Following Eq. (1) for the S/N ratio and to maintain the usual convention of optimization being a minimization process, S/N is negated when used as an objective function. Therefore, $f_1(\boldsymbol{x}, \boldsymbol{u}_i)$ is:

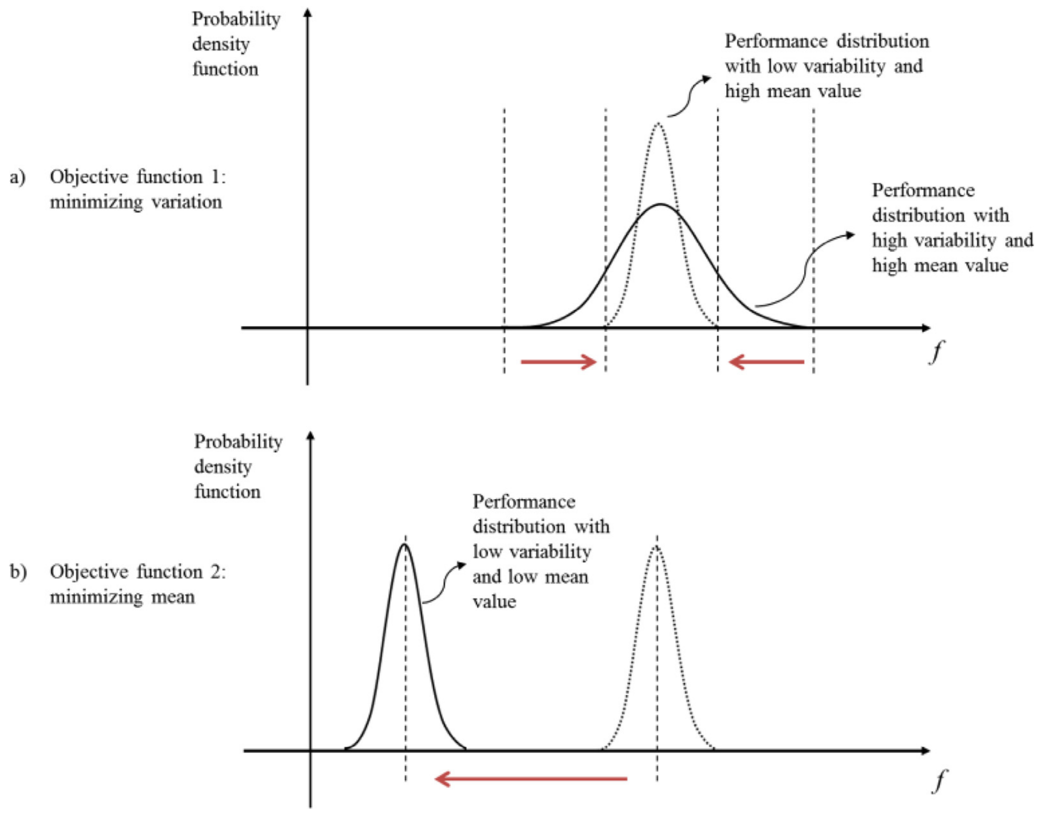


**Fig. 3.** visualization of the designed effects of the two objective functions.

$$f_1(\boldsymbol{x}, \boldsymbol{u_i}) = -10log_{10}\left[\frac{\left(\sum_{i=1}^{p} PE_{TDY(\boldsymbol{u}_1),\boldsymbol{i}}\right)^2}{\boldsymbol{MSD}}\right] \tag{7}$$

$p$ being the temporal resolution of data. For example, p has to be set to 12 where calculating annual energy performance by accumulating 12 monthly values. Furthermore, p has to be set to 8760 where calculating the annual energy performance over hourly values and to 24 where calculating daily energy performance over the 24 h in a day. Minimizing $f_1(\boldsymbol{x}, \boldsymbol{u}_i)$ results in minimizing the sensitivity of the response (energy use) to the variability of noise (climate conditions).

**Objective function n.2**: The purpose of $f_2(\boldsymbol{x}, \boldsymbol{u}_i)$ is to optimize a building's energy use under the most likely climate conditions. The objective functions can be formulated as:

$$f_2(\boldsymbol{x}, \boldsymbol{u_i}) = \sum_{\boldsymbol{i}=1}^{\boldsymbol{p}} PE_{TDY(\boldsymbol{u}_1),\boldsymbol{i}} \tag{8}$$

It is now possible, with the two objectives described above, to conceptualize an RDO process in which climate uncertainty is introduced in simulations as a noise factor using only three weather files. Objective function n.1 minimizes, in this process, the deviation between responses under extreme and average conditions. Objective function n.2 brings the primary energy mean value close to the target value (ideally zero). The above concept is visualized in Fig. 4 for two time steps during a heating period and cooling period.

The above formulation allows robust design optimization to be performed at different temporal resolutions. This feature is required because the effect of a noise factor on the performance variability of a building system varies according to its typical response time. For example, the seasonal effect of climate variation would need to be considered when optimizing building envelope properties. A monthly resolution might therefore be appropriate. The temporal resolution of climate variation may have to be finer, e.g. day or hour, when optimizing building devices such as automated shadings. Two sets of design variables were therefore considered in the development of the optimization process. They are building envelope properties and control settings. Two configurations based on these two groups were designed for the optimization process (see Section 3.4). The energy models and design variables that are considered for this study are described below in Section 3.2 and 3.3 before moving to the formulation of optimization process.

### 3.2. Building models

The commercial reference building models were developed by Pacific Northwest National Laboratory (PNNL), under contract with the U.S. Department of Energy (DOE) [59]. The package includes 16 building type models. These models are provided in three categories: "*new construction*", "*post-1980*″ and "*pre-1980*″ (existing buildings constructed in or after 1980 and before 1980). The *new construction* models are modified according to recent editions of the ASHRAE 90.1 Standard [60]. Detailed descriptions of reference model development and modeling strategies can be found in PNNL's reports [61,62]. The small office building model was used in this study. Two base-cases were considered; one from the *new construction* category complying with the ASHRAE 90.1-2016 standard and one from the *post-1980* category. These cases are called "2016-compliant base-case", which represents a recent new-build building quality and the "1980-compliant base-case" which represents an existing building quality. This allows the energy robustness of models representing newly built and existing older buildings to be assessed under climate uncertainty. This case study also shows the potential improvement that can be achieved by "robustifying" the energy performance of buildings. The reference building models are also categorized based on ASHRAE climate zones [63],

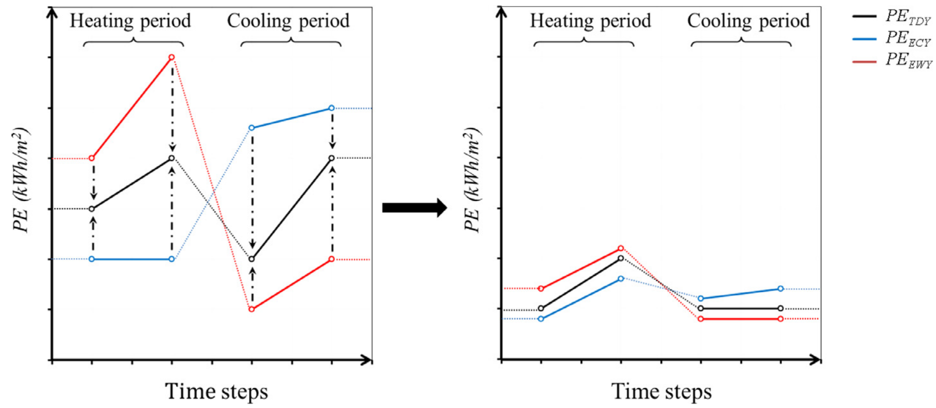


**Fig. 4.** The concept of robust design optimization using three weather files: TDY, ECY and EWY.

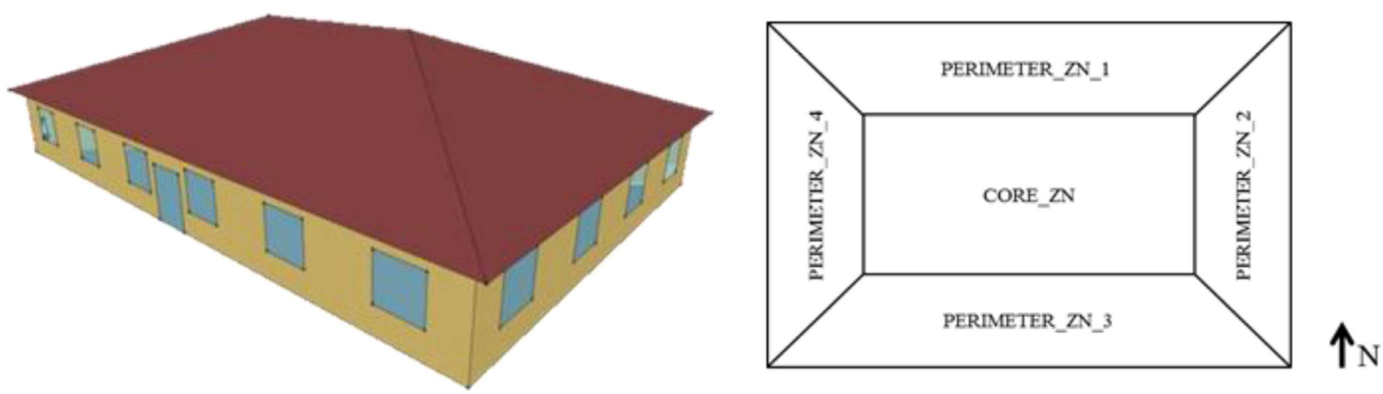


**Fig. 5.** Reference building model geometry and zone planning.

**Table 2**
Description of the thermal zones.

| Zone | Area ($m^2$) | Conditioned (Y/N) | Volume ($m^3$) | Gross wall area ($m^2$) | Window Glass Area | Lighting ($W/m^2$) | People ($m^2$/person) | Number of people | Appliance ($W/m^2$) |
|---|---|---|---|---|---|---|---|---|---|
| CORE_ZN | 149.7 | Yes | 456.5 | 0.0 | 0.0 | 10.8 | 16.6 | 9 | 6.8 |
| PERIMETER_ZN_1 | 113.5 | Yes | 346.1 | 84.5 | 20.6 | 10.8 | 16.6 | 7 | 6.8 |
| PERIMETER_ZN_2 | 67.3 | Yes | 205.3 | 56.3 | 11.2 | 10.8 | 16.6 | 4 | 6.8 |
| PERIMETER_ZN_3 | 113.5 | Yes | 346.1 | 84.5 | 16.7 | 10.8 | 16.6 | 7 | 6.8 |
| PERIMETER_ZN_4 | 67.3 | Yes | 205.3 | 56.3 | 11.2 | 10.8 | 16.6 | 4 | 6.8 |
| Attic | 568.0 | No | 720.3 | 0.0 | 0.0 | 0.0 | – | 0 | 0.0 |
| Total | 511.3 | | 2 279.6 | 281.6 | 59.7 | | | 31 | |

which are classified according to the calculated heating degree-day base 18 °C ($HDD_{18}$) and cooling degree-day base 10 °C ($CDD_{10}$). The 5-year average (2013–2017) of degree-day values were calculated for the Geneve-Cointrin weather station, to find the model that is best suited to Geneva. The calculated values were 2831 for $HDD_{18}$ and 1460 for $CDD_{10}$, which corresponds to the Cold-Humid (5A) ASHRAE climate zone. The base-case models were therefore chosen from the 5A climate zone. A summary of geometry description, thermal zones, envelope properties, and control settings of the building models are given in Fig. 5, Tables 2 and 3.

The dynamic energy simulations of the building models were performed using the EnergyPlus [64] software version 8.5.0. Each version of EnergyPlus released undergoes two major types of validation tests [65]: analytical tests according to ASHRAE Research Projects 865 and 1052, and comparative tests according to the ANSI/ASHRAE 140 [13] and IEA SHC Task34/Annex43 BESTEST method. Heat conduction through the opaque envelope was calculated via the conduction transfer functions (CTF) using a 15-minute time step. The natural convection heat exchange near internal and external surfaces was calculated using the thermal analysis research program (TARP) algorithm [66]. The initialization period of simulation was set to the maximum option, which is 25 days [67]. The primary energy use was calculated by converting the simulation outputs for delivered energy, the conversion factors specified in Swiss norm SIA 380/1:2009 [68] being used to convert delivered energy to primary energy. The factor for converting electricity to primary energy is therefore 2.97 kWhPE/kWhel and for converting natural gas to primary energy it is 1.15 kWhPE/kWhgas.

### 3.3. Design variables for optimization

The input variables considered for the target building were divided into two groups: building envelope properties and control

**Table 3**
Design variables and their ranges for optimization and the values of base-cases.

| Category | Description of variables | Variable names | Unit of measure | Type of variable | 2016-compliant base-case value | 1980-compliant base-case value | Sampling ranges |
|---|---|---|---|---|---|---|---|
| **Properties of the building envelope** | | | | | | | |
| Window properties | *U*-value | X01 | W/(m$^2$ K) | Continuous | 0.41 | 3.35 | [0.20, 5] |
| | SHGC | X02 | – | Continuous | 0.38 | 0.39 | [0.10, 0.90] |
| | Visible transmittance | X03 | – | Continuous | 0.49 | 0.80 | [0.10, 0.90] |
| Roof properties | Solar absorptance | X04 | – | Continuous | 0.70 | 0.92 | [0.10, 0.90] |
| | Thermal resistance | X05 | (m$^2$ K)/W | Continuous | 8.10 | 2.98 | [0.20, 33.20] |
| Wall | Solar absorptance | X06 | – | Continuous | 0.70 | 0.92 | [0.10, 0.90] |
| | Thermal resistance | X07 | (m$^2$ K)/W | Continuous | 3.07 | 1.34 | [0.20, 33.20] |
| Floor | Thermal resistance | X08 | (m$^2$ K)/W | Continuous | 0.22 | 0.22 | [0.20, 33.20] |
| Infiltration | Flow per Exterior Surface Area | X09 | 1/h | Continuous | 0.37 | 1.72 | [0.04, 1] |
| **Daily control settings** | | | | | | | |
| Cooling setpoint | Setpoint temperature | X10 | °C | Discrete | 24 (whole year) | 24 | 24, 24.50, 25…,27 |
| Heating setpoint | Setpoint temperature | X11 | °C | Discrete | 21 (whole year) | 21 | 19, 19.50, 20, 20.5, 21 |
| Shading setpoint | Solar incidence on south window | X12 | W/m$^2$ | Discrete | No shading | No shading | 200, 250, 300…, 1000 |
| | Solar incidence on north window | X13 | W/m$^2$ | Discrete | No shading | No shading | 200, 250, 300…, 1000 |
| | Solar incidence on east window | X14 | W/m$^2$ | Discrete | No shading | No shading | 200, 250, 300…, 1000 |
| | Solar incidence on west window | X15 | W/m$^2$ | Discrete | No shading | No shading | 200, 250, 300…, 1000 |

settings. Building envelope properties can be divided into five categories: window properties, roof properties, wall properties, floor properties, and infiltration. Control settings include cooling, heating and shading setpoints. A total of 15 variables were finally selected. The design variables used for the thermal properties of the building envelope were all assumed to be continuously uniform. The control settings were assumed to be discrete variables with integer values that represent the different assigned information indicated in Table 3.

### *3.4. Formulation of optimization process*

systems are characterized by different response times. A two-step optimization process was therefore designed to identify reliable values for the input variables for the appropriate time effect of the noise factor. A monthly resolution was firstly used for the seasonal effect of climate variation. Annual primary energy was used to optimize building envelope properties. An hourly resolution was, secondly, used for short-term weather evolution, and daily primary energy was used to optimize the building's control settings. For example, maximum irradiance incident on a window was used for lowering automated solar shadings. This two-step optimization process also provides, when designing an energy robust building, an insight into whether it is sufficient to apply only optimal control settings or only apply improving the building envelope, or whether both strategies are important. There may also be an option priority for the two. Deploying optimum control settings of course requires less intervention and cost in the context of building refurbishment, renovation of the building envelope maybe requiring a large capital investment. Two different optimization configurations were therefore developed. The dynamic energy simulation engine EnergyPlus [64] was integrated into the modular environment for process automation and optimization in the engineering design process modeFRONTIER [69]. This embeds a multi-objective optimization engine that integrates a number of optimization algorithms and sampling strategies. Genetic Algorithm (GA) was used in this work for the multi-objective optimization. GA is the most common optimization strategy used in building performance analysis [2]. modeFRONTIER provides both a Fast Non-dominated Sorting Genetic Algorithm (NSGA-II) algorithm [70] and a Multi-Objective Genetic Algorithm (MOGA-II) [71]. MOGA-II is an improved version of MOGA [72]. Both the algorithms were used in the first optimization process with a similar initial population to determine which optimization algorithm is best suited to the process. MOGA-II provided better results and was chosen for the second optimization process.

The multi-objective optimization process results in a two-dimensional solution space with a Pareto frontier. Fig. 6 demonstrates the strategy used in this study for post-processing and selecting the Pareto optimal. The Pareto frontier is, in this method, normalized to zero-one interval ($0 \le f_i^t(x) \le 1$) using the following transformation [73]:

$$f_i^t(x) = \frac{f_i(x) - f_i^{min}}{f_i^{max} - f_i^{min}} \tag{9}$$

$f_i^{max}$ and $f_i^{min}$ are the maximum and minimum of $f_i(x)$, $x \in \mathbb{R}^s$. The closest point to the utopia point ($f_1 = 0$ and $f_2 = 0$) was then chosen as the optimal solution. This method was used because the significance of both objective functions was considered to be equal and because the values of the two objective functions were expressed at different orders of magnitude.

**Configuration no.1: optimization of the building envelope**

Only the input variables related to thermal properties of the building envelope are, in this task, optimized for robustness. The weather file used for running the simulation was the noise factor that was applied. Two different weather files were used to represent the extreme climate conditions, EWY and ECY. The optimization process was performed for both NSGA-II and MOGA-II. The parameter settings of the algorithms are important to their performance. Hamdy et al. [74] recommended that the minimum number of evaluations required for optimization of building energy models is 1400–1800. The population size for population-based optimizations is recommended to be 2–4 times the number of design variables [75]. Following these recommendations, 1620 evaluations were considered for each algorithm using a population size of 27 ($3 \times 9$ design variables), the number of generations being 60. The initial population was generated based on a random sequence. The default values for the other settings were kept unchanged. These settings are reported in Table 4. Three energy simulations were run in each evaluation (using the EWY, ECY and TDY files) to calculate the two objective functions in Eq. (7) and Eq. (8).

The workflow in Fig. 7 was set up in modeFRONTIER to perform the above optimizations. The flowchart illustrates the flow of information.

The second process aims to optimize the daily control setting using TDY, ECY and EWY. The process is based on typical hourly and extreme values (see Section 2.2). This configuration, unlike the first configuration, excludes the input variables related to thermal properties of the building envelope. Only the control settings are therefore considered in the optimization run. The same noise used in configuration no.1 is used in no. 2. The optimization was performed for each day of the year using the MOGA_II algorithm. The number of evaluations in this run is 48, the probability of directional cross-over and the probability of mutation being kept the same as the previous configuration. The initial population of 6 designs is generated using a random sequence. The number of generations is set to 8. These values were set using trial and error to find a process with an acceptable convergence level and feasible time. Fig. 8 presents an optimization evolution for one day as an example. For each evaluation, 3 energy simulations were run under the three weather files. A total of 365 optimizations were therefore performed to find optimum control settings for each day of the year. Objective functions were set according to Eq. (7) ($p = 24$) and Eq. (8). The last solution of each optimization is considered to be the optimum control setting for that day.

Fig. 9 demonstrates the flowchart of the optimization process for the above configuration.

### *3.5. Evaluating the main effect of the design variables on the objective functions*

A screening analysis tool implemented in modeFRONTIER allows the main and interaction effects of design variables on a response to be evaluated [76]. The tool is based on the Smoothing Spline ANOVA (SS-ANOVA) method that is suitable for multivariate modeling and regression problems [76,77]. SS-ANOVA is a statistical modeling algorithm based on a function decomposition that is similar to the classical analysis of variance (ANOVA) decomposition [76]. Global variance is explained (decomposed) through this method into single model terms in a statistical model. I.e., the percentage of its contribution to the global variance is calculated for each design variable. The 1620 evaluations in the first optimization process were used as a dataset in a sensitivity analysis to determine the relative importance of the design variables on the two objective functions. The results of the analysis indicate the percentage of each variable's contribution to: 1) the variability in primary energy use (objective function No.1) and, 2) the mean value of primary energy use (objective function No.2).

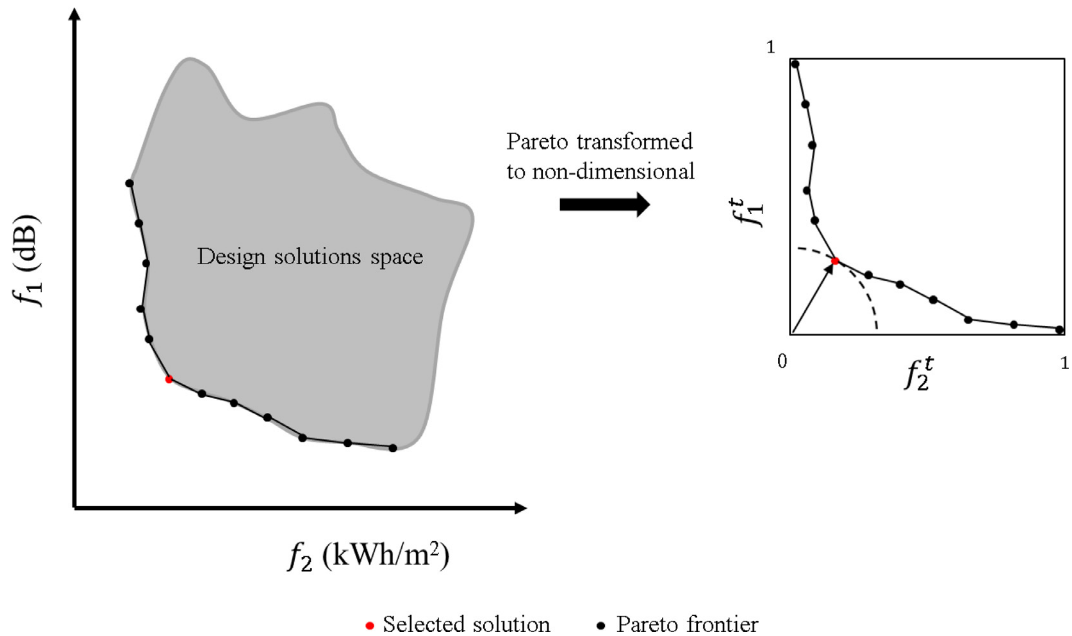


**Fig. 6.** The approach for selection of the best solution from the Pareto.

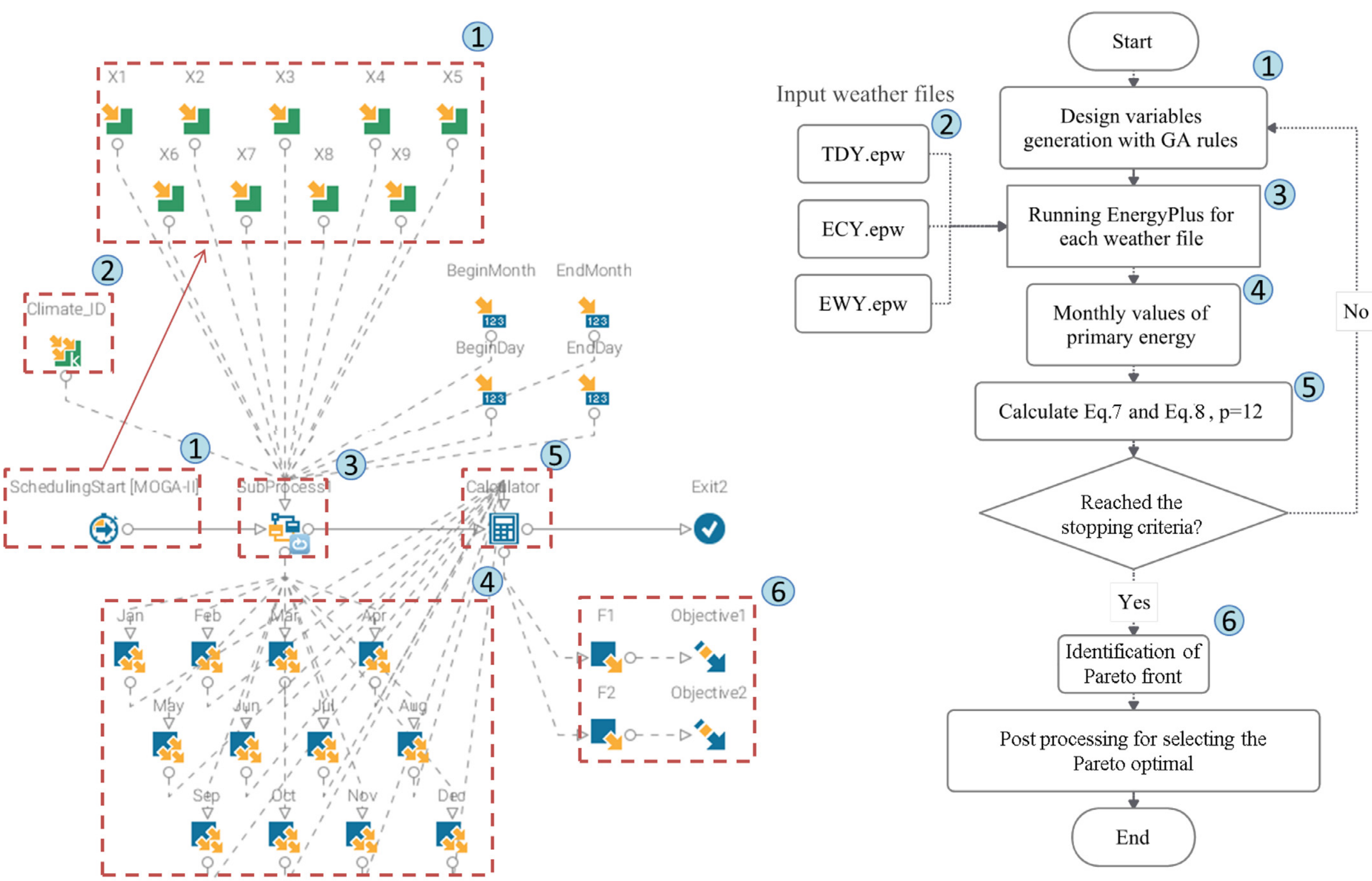


**Fig. 7.** The implemented workflow of optimization process in modeFRONTIER for configuration no.1. The flowchart describes the flow of information during the process. Configuration no.2: optimization of the control settings.

**Table 4**
Parameter settings the selected optimization algorithms.

| Optimization algorithm | No. of evaluations | Simulation resolution | *p* | No. of runs | Population size | No. of generations | Probability of cross-over | Probability of mutation |
|---|---|---|---|---|---|---|---|---|
| NSGA-II | 1620 | Monthly | 12 | 1 | 27 | 60 | 0.9 | 1.0 |
| MOGA-II | 1620 | Monthly | 12 | 1 | 27 | 60 | 0.5 | 0.1 |

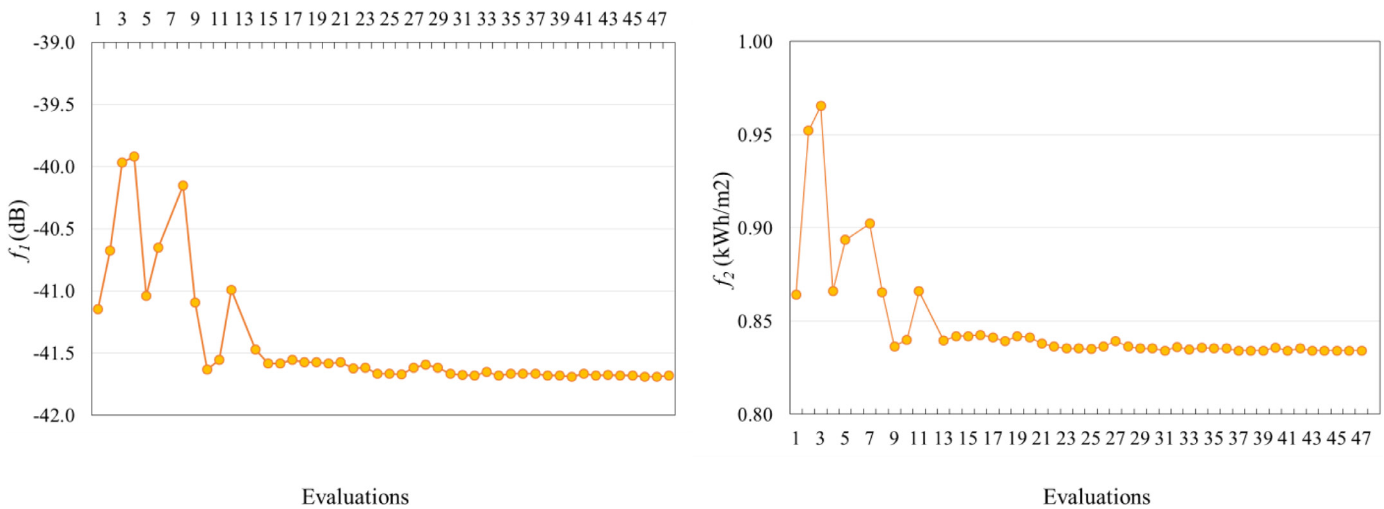


**Fig. 8.** Evolution of objective functions. Example of optimizing control settings for a day.

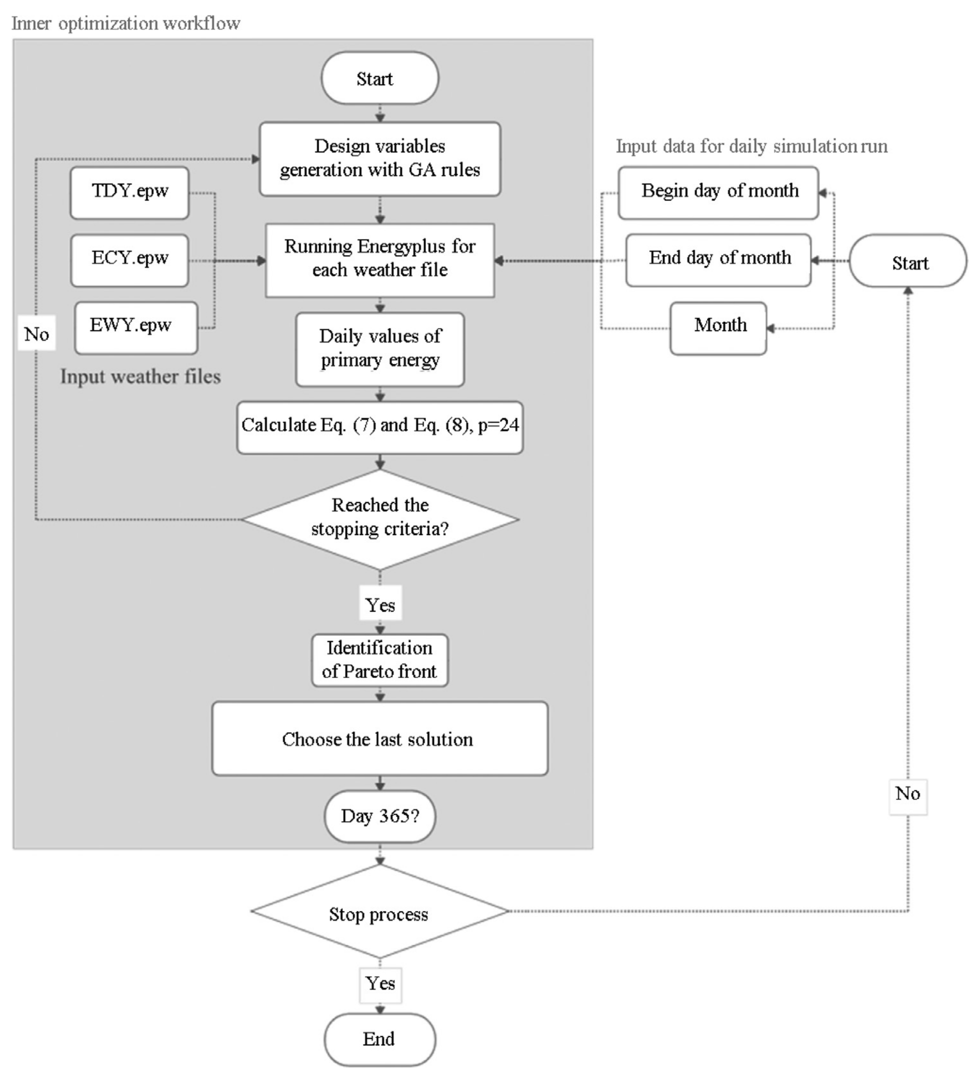


**Fig. 9.** Flowchart of the optimization process implemented in modeFRONTIER for configuration no.2.

### 3.6. Assessment of optimization strategies

Six cases were designed to assess the impacts of each group of design variables on the energy robustness of buildings under climate change:

1. *2016-base*: This is the 2016-compliant base-case model with fixed heating and cooling setpoint values and no automated solar shadings.

Three cases were developed to identify the most effective optimization strategy:

2. *2016-EnvelopeOpt:* Envelope properties of the 2016-base model optimized using configuration no.1. Control settings are not optimized and remain the same as for the 2016-base.
3. *2016-ControlOpt:* Configuration no.2 used in the optimization process. The control settings were optimized. The envelope property values were fixed and equal to the 2016-base model. Automated solar shading is added to the 2016-base model and optimum daily *values* are used for setting the setpoint values for space heating and cooling and solar shading control.
4. *EnvelopeOpt+ControlOpt:* Envelope property values were as for the solution 2016-EnvelopeOpt. Configuration no.2 was used for the optimization of control settings.

The building that we assumed was compliant with 1980s quality standards was then used in optimization.

5. *1980-base:* This building model has the same geometry as the 2016-base, but has a construction that is set to typical 1980s quality standards.

It should be noted that only optimizing the building envelope without upgrading the HVAC systems may not be comply with the latest legislative requirements (e.g. in Europe the Energy Performance of Buildings Directive). It may also not be compatible with the lifecycle of an HVAC system, which is not more than 30 years. Renovating a 1980-compliant base-case building by upgrading the HVAC systems to recent requirements (let's say 2016) and optimizing the building envelope to maximize its energy-robustness and energy-efficiency gives the *2016-EnvelopeOpt*. Furthermore, optimizing the envelope properties and the control settings gives the *EnvelopeOpt+ControlOpt*. We therefore study the case in which an existing building is enhanced by optimizing its control settings, which requires a low level of investment.

An additional case was therefore studied:

6. *1980-ControlOpt:* Configuration no.2 was considered for the optimization process. The control settings were optimized. Envelope property values fixed and equal to the 1980-base model. Automated solar shading was added, optimum daily values used for setting the setpoint values for space heating and cooling and solar shading control.

## 4. Robustness evaluation

All the above 6 cases were tested against a weather file dataset of 74 representative weather files generated for the city of Geneva, to test the effectiveness of the proposed method and demonstrate the most energy-robust building variant to climate change. The set of the representative weather files was synthesized in a previous study [56]. The synthesis was carried out to determine both extreme and typical climate conditions that represent a suitable test bench for investigating the energy performance of a building under changing climate. The weather files are divided into three groups:

- TMY group: includes two weather files, the IWEC typical meteorological year (TMY) and a TMY generated by Meteonorm
- Statistical group: six weather files generated using the morphing method by CCWorldWeatherGen and WeatherShift, and three weather files generated using the stochastic method by Meteonorm
- Dynamical group: 21 weather files generated using dynamical downscaling and that represent typical conditions and 42 weather files generated using dynamical downscaling and that represent extreme conditions.

Typical weather files refer to the files that are generated through statistical downscaling or dynamical downscaling (TDY series). Extreme weather files refer to ECY and EWY files that represent extreme cold and warm years (using the RCM dynamically downscaled data). All the above methods provide 72 future weather files for the city of Geneva. More details are provided in [56].

This assessment methodology was applied to identify the most effective optimization strategy that can give a new building a robust energy performance under climate change and measure the robustness potential.

## 5. Results

The first optimization round was performed to find optimal values for the building envelope properties (2016-EnvelopeOpt). The optimization parameters were set as described in Section 3.4. Fig. 10 shows the scatterplot of the simulated building variants using MOGA_II and NSGA_II algorithms. MOGA_II demonstrates better performance by covering a larger area of the design space and providing a Pareto frontier closer to the utopia point.

The optimal solution is selected from the Pareto frontier using the approach described in Section 3.4. The Pareto frontier is, in this approach, first normalized to values between zero and one, the solution with minimum distance to the ideal point then being selected as the optimal solution. The normalized Pareto frontier and the selected solution are shown in Fig. 11.

Table 5 presents the values of the optimal solution (2016-EnvelopeOpt) and compares them with the values of building envelope properties for the 2016-base and 1980-base cases.

A built-in tool from modeFRONTIER was used to calculate the contribution of each variable to the objective functions (as described in Section 3.5), to better understand the importance of each variable on the variability and mean of primary energy use. The analysis was conducted on the dataset generated from the optimization process with 1620 evaluations using MOGA_II algorithm. The tool created two statistical models of the global variance for objective function No.1 and No.2 from which the main effects of each variable were derived as a percentage (contribution index). The reported values for the R-squared (coefficient of determination) of the models were 0.958 for objective function No.1 and 0.933 for No.2. R-squared is a statistical measure of how well the regression model approximates the data, and therefore provides information on the goodness of fit of the model [76]. An R-squared of 1 indicates a perfect fit. The results of this analysis are shown in Fig. 12.

Fig. 12 shows that the variance in objective function No.1 is mainly influenced by the window SHGC (X02), roof thermal resistance (X05) and floor thermal resistance (X08) input variables. The variables that exercise the greatest influence on objective function No.2 are window U-value (X01), roof thermal resistance (X05) and wall thermal resistance (X07). The results reveal that, for the city of Geneva, window SHGC plays a significant role in the sensitivity of the building's energy performance to outdoor climate conditions. The thermal properties of windows and roof of buildings are, for this city, the key design variables for improving the energy-robustness of buildings to climate change.

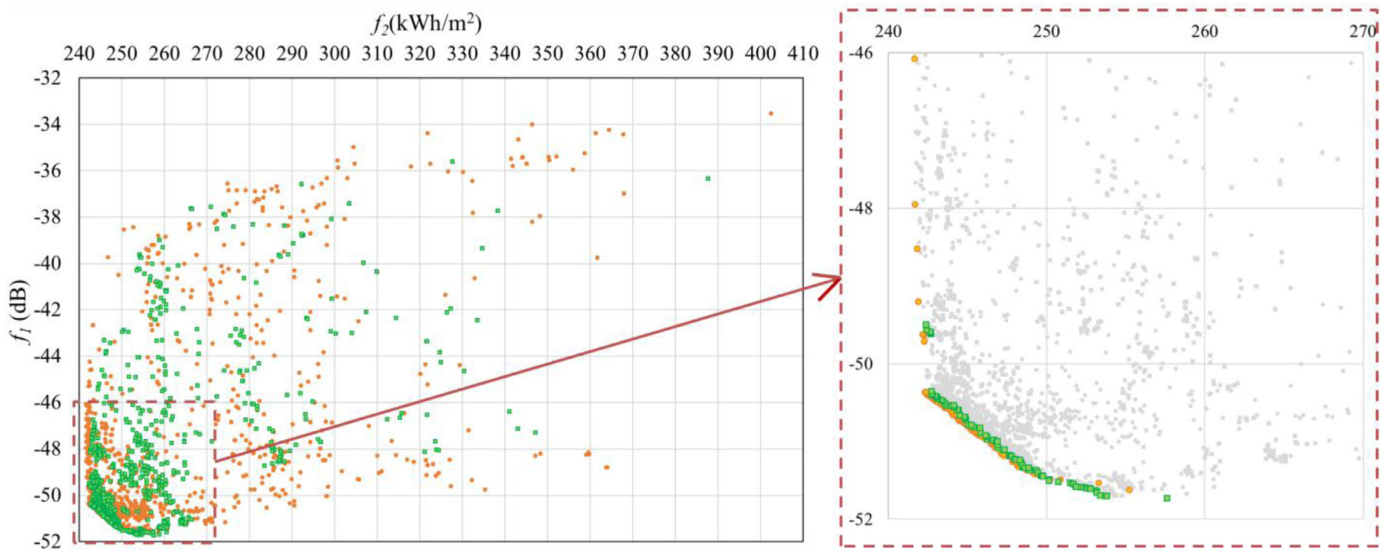


**Fig. 10.** Scatter plot for the optimization of building envelope properties (in orange are building variants using MOGA_II algorithm and in green the ones based on NSGA_II algorithm).

**Table 5**
comparison of the optimal values for the building envelope properties (2016-EnvelopeOpt) with 2016-base and 1980-base cases values.

| Variable names | Description of variables | Unit of measure | 2016-base | 1980-base | 2016-EnvelopeOpt |
|---|---|---|---|---|---|
| X01 | Window *U*-value | W/(m² K) | 0.41 | 3.35 | 0.20 |
| X02 | Window SHGC | – | 0.38 | 0.39 | 0.10 |
| X03 | Window visible transmittance | – | 0.49 | 0.80 | 0.69 |
| X04 | Roof solar absorptance | – | 0.70 | 0.92 | 0.31 |
| X05 | Roof thermal resistance | (m² K)/W | 8.10 | 2.98 | 33.20 |
| X06 | Wall solar absorptance | – | 0.70 | 0.92 | 0.10 |
| X07 | Wall thermal resistance | (m² K)/W | 3.07 | 1.34 | 33.20 |
| X08 | Floor thermal resistance | (m² K)/W | 0.22 | 0.22 | 0.24 |
| X09 | Infiltration | 1/h | 0.37 | 1.72 | 0.04 |

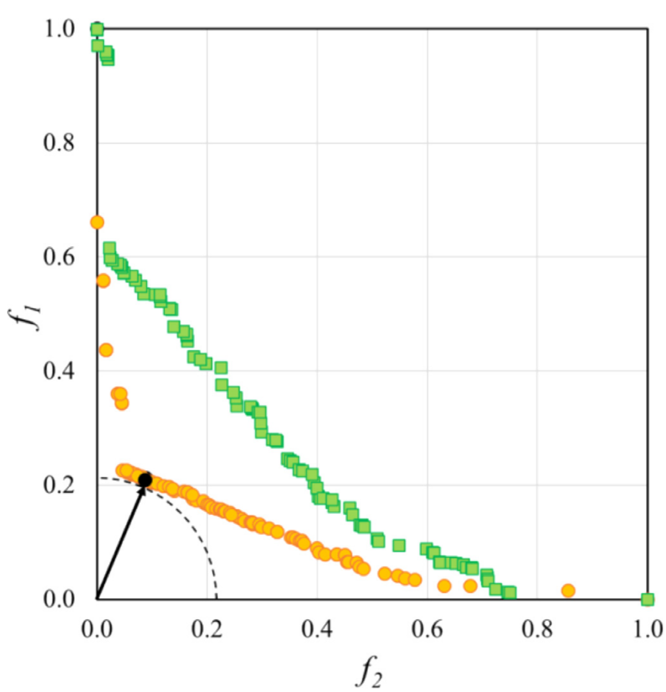


**Fig. 11.** Normalized Pareto frontier with the selected optimal solution in black (in orange are normalized Pareto frontier using MOGA_II algorithm and in green the ones provided by NSGA_II algorithm).

The next step is to find solutions for 2016-ControlOpt, EnvelopeOpt+ControlOpt and 1980-ControlOpt using optimization configuration no.2. This configuration allows optimum daily values for heating, cooling and shading setpoints to be found. The 2016-ControlOpt case finds the optimum values with envelope properties remaining as for the 2016-base case. This process was also applied to the 1980-ControlOpt case by keeping envelope properties as for the 1980-base case. The EnvelopeOpt+ControlOpt case finds these values with the optimum building envelope properties set as for the 2016-EnvelopeOpt. This step is a combination of configuration no.1 and no.2. The above-mentioned process provides solutions for the configuration of the six cases described in Section 3.5. The robustness to climate change of the six cases were assessed after performing all the optimizations. Each case underwent 74 annual simulations using 74 representative weather files (described in Section 4).

Fig. 13 shows the results of this assessment. These are the distribution of 74 primary energy values calculated for each case under 74 different weather files, which includes typical and extremes. This shows that the primary energy use of the 1980-base case has the highest sensitivity to changing climate by a significant margin. Sensitivity in falling order is 1980-ControlOpt, 2016-base, 2016-EnvelopeOpt, 2016-ControlOpt and EnvelopeOpt + ControlOpt. The statistics that are based on the 74 primary energy values calculated for each case are presented in Table 6. The relative change (%) of mean and standard deviation (SD) of all cases are compared on the right side of the table with values for the 1980-base and 2016-base cases.

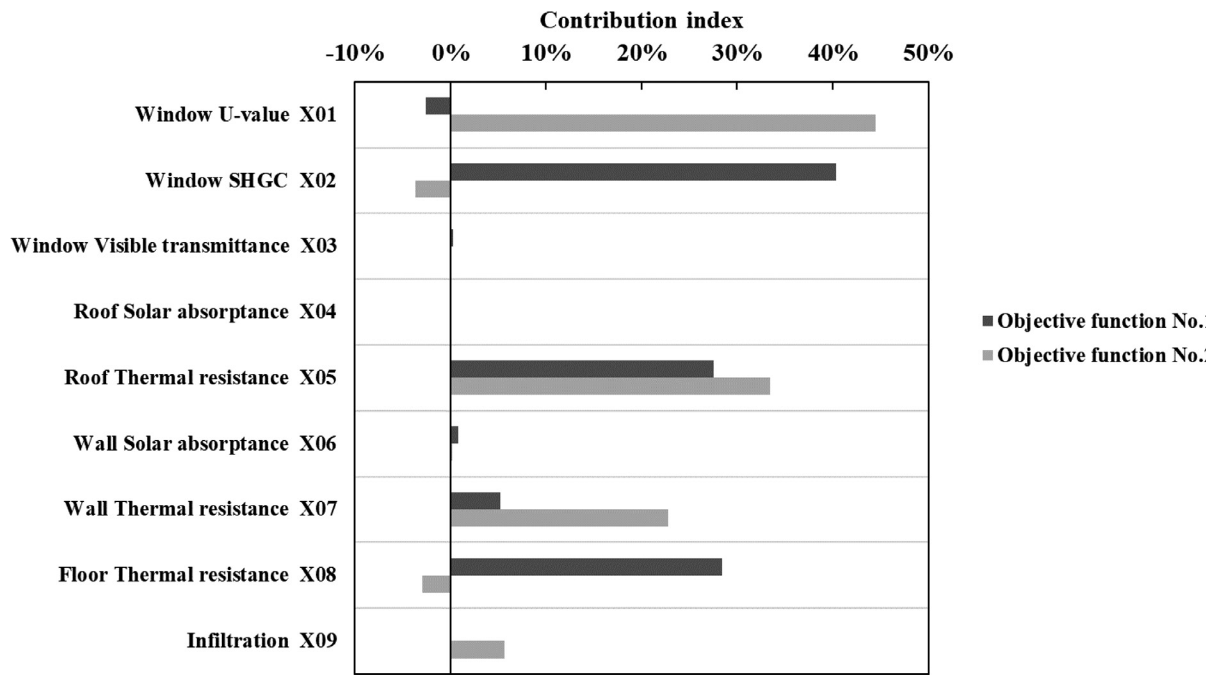


**Fig. 12.** The effects bar chart of contribution indices shows the relative importance of different design variables, that is the percentage contribution of each variable to the global variance of each objective function.

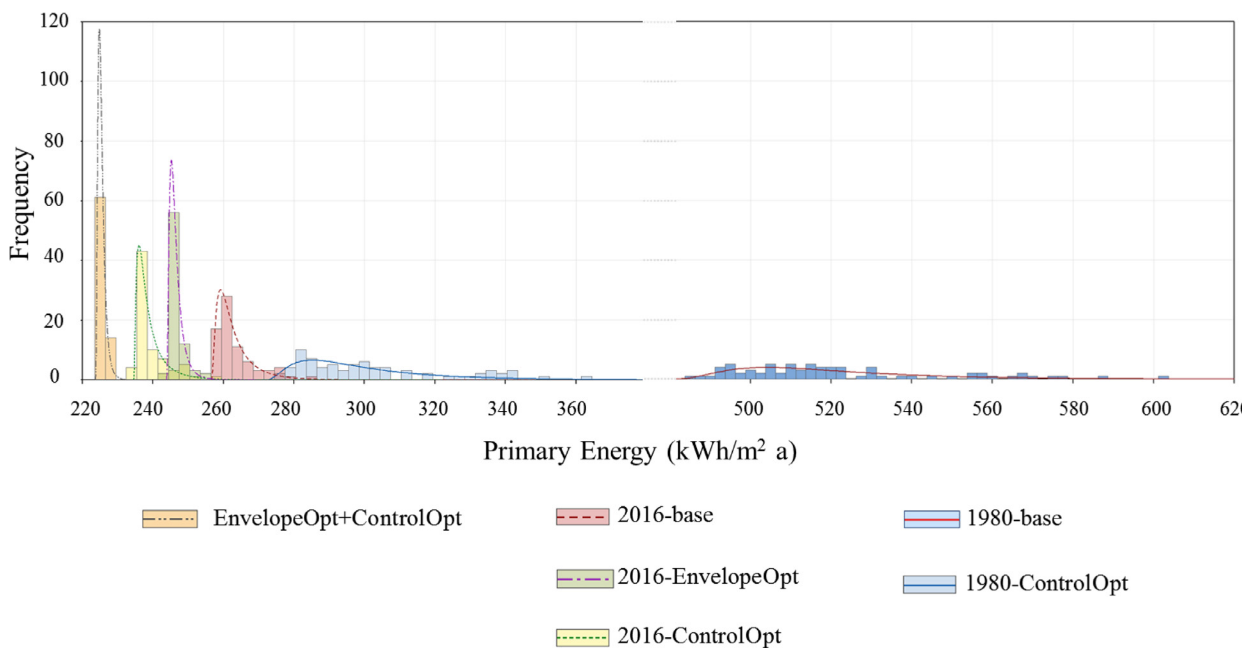


**Fig. 13.** Qualitative distributions comparison of the six cases. For better readability, the distribution of 1980-base is separated from other cases.

**Table 6**
Descriptive statistics based on 74 calculated primary energy use for each case.

| Cases | Primary energy use (kWh/m$^2$) | | | | | Relative Change (%) to 1980-base value | | Relative Change (%) to 2016-base value | |
|---|---|---|---|---|---|---|---|---|---|
| | Mean | SD | Min | Median | Max | Mean | SD | Mean | SD |
| 1980-base | 521.7 | 26.3 | 485.1 | 514.7 | 602.4 | 0.0% | 0.0% | 98.1% | 354.5% |
| 1980-ControlOpt | 301.8 | 21.4 | 275.4 | 296.5 | 363.5 | −42.1% | −18.7% | 14.6% | 269.6% |
| 2016-base | 263.4 | 5.8 | 257.1 | 260.7 | 284.0 | −49.5% | −78.0% | 0.0% | 0.0% |
| 2016-ControlOpt | 239.4 | 4.6 | 234.9 | 237.5 | 257.1 | −54.1% | −82.4% | −9.1% | −19.9% |
| 2016-EnvelopeOpt | 246.7 | 2.1 | 244.2 | 246.2 | 254.6 | −52.7% | −92.1% | −6.3% | −64.0% |
| EnvelopeOpt + ControlOpt | 225.5 | 1.1 | 223.9 | 225.1 | 228.9 | −56.8% | −95.9% | −14.4% | −81.5% |

Looking deeper into the results, the distribution of 2016-CotrolOpt has a lower mean than the 2016-EnvelopeOpt but has a longer tail that covers the distribution of the 2016-EnvelopeOpt case. This means that the EnvelopeOpt case has a higher energy demand than the 2016-CotrolOpt case, but that the demand is more predictable under extreme conditions. Comparing the 1980-base and 1980-ControlOpt shows that optimum control settings cause a significant reduction in the mean primary energy use. Variation, however, remains significantly high and is unreliable during extreme climate conditions. The highest value of the 1980-CotrolOpt case is, however, still lower than the lowest value of 1980-base case. This means a significant improvement can be achieved by only applying the minimum intervention of optimum control settings. The EnvelopeOpt+ControlOpt case has a very narrow distribution compared to the other cases and also the lowest mean value.

The statistics in Table 6 show that the calculated standard deviation for the EnvelopeOpt+ControlOpt case is around 5 times (81.5%) smaller than 2016-base case and is almost 24 times (95.9%) smaller than 1980-base case. This points to a significant reduction of variability in primary energy use. This is in addition to having the lowest mean value of primary energy use. This makes the EnvelopeOpt+ControlOpt case not only the most energy-efficient case, but also the case with most robust energy performance. It demonstrates the effectiveness of the proposed method for designing buildings with robust energy performance under future climate uncertainties.

The results furthermore show that shading and control settings have the highest impact on energy-efficiency. In other words, adjusting the cooling and heating setpoints to optimum values and including the solar incident setpoint for shading gives a significant reduction in primary energy use under typical conditions. Optimizing building envelope properties effectively reduces $f_1$, and gives a solution that has a lower variability in its response to extreme conditions and therefore better energy performance robustness.

## 6. Conclusions

This paper provides an account of a number of available technologies. These include building performance simulation tools, simulation-based optimization techniques, robust design approaches and climate model data. The paper then describes a method that is based on a combination of these that allow the design of buildings with a more robust and efficient energy performance in the face of climate change. The main goal of this study was to provide a computationally feasible and easy to understand method that can be used effectively by building designers, architects and engineers to improve the robustness of their designs to future climate uncertainties.

Our work, in summary, proposes a robust design optimization (RDO) workflow. The aim of this is to achieve an optimum solution and its energy performance which has a minimum sensitivity to climate variations. The key to the method's feasibility is considering climate variations using only three weather files. These are typical (TDY), extreme warm (EWY) and extreme cold (ECY) weather conditions. A multi-objective optimization process was configured with two objective functions. Minimization of objective functions ensures a building with low energy use under the most likely conditions and with minimum variance under disturbances or extreme events. Building envelope properties of the 2016 compliant model (2016-base case) were optimized in the first step. The optimum solution selected is called 2016-EnvelopeOpt (Fig. 10). Building envelope properties of the 2016-base case were unchanged in the second step. Shading was, however, added, and the daily control setting of heating, cooling and shading were optimized. The solution from this step is called 2016-ControlOpt. This process was performed on the 1980 compliant model (1980-base case).The envelope properties were unchanged and control settings were optimized and presented as 1980-ControlOpt.

Comparing the acquired results allows:

- The impact of different interventions on the energy-robustness of a building to be better understood, interventions ranging from deep and costly interventions such as to envelope properties to less costly interventions such as shading and control settings.
- The impact of such interventions to be shown for a building that is built according to a recent energy code, and for a building that is built to a 1980s construction quality.

In the final step, optimization was performed to find optimum control settings for heating, cooling and shading for the optimum envelope properties case (2016-EnvelopeOpt case). This resulted in the EnvelopeOpt + ControlOpt case, in which both envelope properties and control settings are optimized.

The results demonstrate that optimum daily setpoint temperatures for cooling and heating, and solar incident setpoint for shading, allows a significant reduction in primary energy use under typical conditions (2016-ControlOpt and 1980-ControlOpt cases). Optimizing the building envelope properties (2016-EnvelopeOpt) furthermore significantly reduces the variability of performance under changing climate conditions, including extreme conditions. Finally, optimizing both envelope properties and the control settings achieves the most energy-efficient solution with a robust energy performance (EnvelopeOpt + ControlOpt case). This case has a considerably lower sensitivity to climate conditions by having low-variability performance, and also minimum energy use.

## 7. Future works

The simplicity and the low computational demand of the process underlies the feasibility and applicability of this method. The approach can be used at any stage of the design process and can help architects and engineers improve the robustness of their design to future climate uncertainties. This study has only examined the method on a reference building in the city of Geneva. Applying this method to other locations and to different types of buildings can therefore give a deeper knowledge of designing future buildings with robust performance. The approach used in this study can also be used as a guideline to develop further robust design optimization (RDO) processes for other significant noise factors than climate (e.g. occupant behavior) and other target performances than energy (e.g. indoor environmental qualities). We are currently in the process of investigating an RDO in which both climate and occupant behavior are a source of variations. We believe that our research will also serve as a basis for future studies at the urban scale, where robustness of built environment to climate change impacts are crucial.

## Declaration of Competing Interest

We wish to confirm that there are no known conflicts of interest associated with this publication and there has been no significant financial support for this work that could have influenced its outcome.

We confirm that the manuscript has been read and approved by all named authors and that there are no other persons who satisfied the criteria for authorship but are not listed. We further confirm that the order of authors listed in the manuscript has been approved by all of us.

We confirm that we have given due consideration to the protection of intellectual property associated with this work and that there are no impediments to publication, including the timing of publication, with respect to intellectual property. In so doing we confirm that we have followed the regulations of our institutions concerning intellectual property.

## Acknowledgement

This work has been written within the Research Centre on Zero Emission Neighborhoods in Smart Cities (FME ZEN). The authors gratefully acknowledge the support of the ZEN partners and the Research Council of Norway. This work has partly benefited from the support of the Swedish Research Council (Formas) which is gratefully acknowledged.

## References

[1] W.-J. Suh, C.-S. Park, D.-W. Kim, Heuristic vs. meta-heuristic optimization for energy performance of a post office building, 12th Conference of International Building Performance Simulation Association, 2011.
[2] A.-T. Nguyen, S. Reiter, P. Rigo, A review on simulation-based optimization methods applied to building performance analysis, Appl. Energy 113 (2014) 1043–1058.
[3] R. Evins, A review of computational optimisation methods applied to sustainable building design, Renew. Sustainable Energy Rev. 22 (2013) 230–245.
[4] S. Attia, Computational Optimisation for Zero Energy Building Design, Interviews with Twenty Eight International Experts, Architecture et Climat, 2012.
[5] A.C. Menezes, et al., Predicted vs. actual energy performance of non-domestic buildings: using post-occupancy evaluation data to reduce the performance gap, Appl. Energy 97 (2012) 355–364.
[6] K. Bartlett, et al., Do our green buildings perform as intended, World Sustainable Building Conference (SBE2014), 2014.
[7] P. Li, T.M. Froese, G. Brager, Post-occupancy evaluation: state-of-the-art analysis and state-of-the-practice review, Build. Environ. 133 (2018) 187–202.
[8] G. Iaccarino, Quantification of uncertainty in flow simulations using probabilistic methods, Institute For Computational Mathematical Engineering, Stanford University, 2008.
[9] P. Rastogi, On the Sensitivity of Buildings to Climate - the Interaction of Weather and Building Envelopes in Determining Future Building Energy Consumption, EPFL, 2016.
[10] IEC, 60050-191: International Electrotechnical vocabulary: Chapter 191: Dependability and Quality of Service, International Electrotechnical Commission, Geneva, 1990.
[11] B. Bordass, Energy performance of non-domestic buildings: closing the credibility gap, in: Proceedings of the 2004 Improving Energy Efficiency of Commercial Buildings Conference, Citeseer, 2004.
[12] C.J. Hopfe, Uncertainty and sensitivity analysis in building performance simulation for decision support and design optimization, Eindhoven University of Technology, 2009.
[13] ANSI/ASHRAE 140, in: Standard Method of Test for the Evaluation of Building Energy Analysis Computer Programs, American Society of Heating, Refrigerating and Air-Conditioning Engineers, Atlanta (GA), USA, 2011, p. 272.
[14] Y. Ham, M. Golparvar-Fard, Mapping actual thermal properties to building elements in gbXML-based BIM for reliable building energy performance modeling, Automation in Construction 49 (2015) 214–224.
[15] Y. Ham, M. Golparvar-Fard, *EPAR*: energy performance augmented reality models for identification of building energy performance deviations between actual measurements and simulation results, Energy Build. 63 (2013) 15–28.
[16] W. Pan, A.G.F. Gibb, A.R.J. Dainty, Strategies for integrating the use of off-site production technologies in house building, J. Constr. Eng. Manag. 138 (11) (2012) 1331–1340.
[17] E. Delzendeh, et al., The impact of occupants' behaviours on building energy analysis: a research review, Renew. Sustainable Energy Rev. 80 (2017) 1061–1071.
[18] I.J. Hall, et al., Generation of a typical meteorological year, Analysis For Solar Heating and Cooling, Sandia Labs., Albuquerque, NM (USA), San Diego, CA, USA, 1978.
[19] Kalkman, A., *Calculation of energy consumption in dwellings: theory and field data, presented at the one day forum of the "5th meeting of IEA Annex 53", Rotterdam, The Netherlands,* 2012.
[20] Taguchi, G., *Introduction to quality engineering: designing quality into products and processes*. 1986.
[21] A. Lanzotti, Robust design of car packaging in virtual environment, Int. J. Interact. Des. Manufacturing (IJIDeM) 2 (1) (2008) 39–46.
[22] F. Blaabjerg, M.M. Pecht, Special issue on robust design and reliability of power electronics, ieee transactions on power electronics, may 2015, IEEE Trans. Power Electron. 30 (5) (2015) 2373–2374.
[23] N. Truong, et al., Robust design with time-oriented responses for regenerative medicine industry, The Third International Conference on the Development of Biomedical Engineering in Vietnam, Springer, 2010.
[24] J.L.A. Koolen, Simple and robust design of chemical plants, Comput. Chem. Eng. 22 (1998) S255–S262.
[25] D.B. Crawley, L.K. Lawrie, Rethinking the TMY: is the 'typical'meteorological year best for building performance simulation? 14th Conference of International Building Performance Simulation Association, 2015.
[26] F. Sévellec, S.S. Drijfhout, A novel probabilistic forecast system predicting anomalously warm 2018-2022 reinforcing the long-term global warming trend, Nat. Commun. 9 (1) (2018) 3024.
[27] X. Ke, et al., Quantifying impacts of heat waves on power grid operation, Appl. Energy 183 (2016) 504–512.
[28] R. Kaiser, et al., The effect of the 1995 heat wave in chicago on all-cause and cause-specific mortality, Am. J. Public Health 97 (Suppl 1) (2007) S158–S162.
[29] A. De Bono, et al., Impacts of Summer 2003 Heat Wave in Europe, United Nations Environment Programme, 2004 Retrieved from https://www.unisdr.org/files/1145_ewheatwave.en.pdf .
[30] G. Luber, M. McGeehin, Climate change and extreme heat events, Am. J. Prev. Med. 35 (5) (2008) 429–435.
[31] G. Taguchi, S. Chowdhury, S. Taguchi, Robust engineering: Learn How to Boost Quality While Reducing Costs & Time to Market, McGraw-Hill Professional Pub, 2000.
[32] W.Y. Fowlkes, C.M. Creveling, Engineering Methods for Robust Product Design: Using Taguchi Methods in Technology and Product Development, Addison-Wesley Publishing Company, 1995.
[33] S. Floricel, R. Miller, Strategizing for anticipated risks and turbulence in large-scale engineering projects, Int. J. Project Manag. 19 (8) (2001) 445–455.
[34] D.P. Clausing, Total quality development, Mechanical Eng. 116 (3) (1994) 94.
[35] A. Olewnik, et al., A framework for flexible systems and its implementation in multiattribute decision making, J. Mechanical Design 126 (3) (2004) 412–419.
[36] R.A. Bates, et al., Achieving robust design from computer simulations, Qual. Technol. Quant. Manag. 3 (2) (2006) 161–177.
[37] S.D. Gribble, Robustness in complex systems, in: Hot Topics in Operating Systems, 2001. Proceedings of the Eighth Workshop on, IEEE, 2001.
[38] A.A. Yassine, Investigating product development process reliability and robustness using simulation, J. Eng. Design 18 (6) (2007) 545–561.
[39] R.A. Bettis, M.A. Hitt, The new competitive landscape, Strateg. Manag. J. 16 (S1) (1995) 7–19.
[40] M.J. Chalupnik, D.C. Wynn, P.J. Clarkson, Comparison of ilities for protection against uncertainty in system design, J. Eng. Design 24 (12) (2013) 814–829.
[41] M.S. Phadke, Quality Engineering Using Robust Design, Prentice Hall PTR, 1995.
[42] T. Buso, et al., Occupant behaviour and robustness of building design, Build. Environ. 94 (2015) 694–703.
[43] V. Fabi, et al., Robustness of Building Design With Respect to Energy Related Occupant Behaviour, IBPSA, Chambery, France, 2013.
[44] J.L. Leyten, S.R. Kurvers, Robust Indoor Climate Design, ISIAQ, 2011.
[45] M. Palme, et al., Energy consumption and robustness of buildings, in: Proceedings of the CESB10 Conference, 2010.
[46] M. Palme, A. Isalgué, H. Coch, Avoiding the possible impact of climate change on the built environment: the importance of the building's energy robustness, Buildings 3 (1) (2013) 191–204.
[47] G. Chinazzo, P. Rastogi, M. Andersen, Robustness assessment methodology for the evaluation of building performance with a view to climate uncertainties, in: Proceedings of BS 2015, 2015.
[48] P. Hoes, et al., User behavior in whole building simulation, Energy Build. 41 (3) (2009) 295–302.
[49] W. O'Brien, Occupant-proof buildings: can we design buildings that are robust against occupant behaviour, 13th Conference of International Building Performance Simulation Association, 2013.
[50] R. Kotireddy, P.-J. Hoes, J.L.M. Hensen, A methodology for performance robustness assessment of low-energy buildings using scenario analysis, Appl. Energy 212 (2018) 428–442.
[51] G.-J. Park, et al., Robust design: an overview, AIAA J. 44 (1) (2006) 181–191.
[52] B.L. Gorissen, I. Yanıkoğlu, D. den Hertog, A practical guide to robust optimization, Omega (Westport) 53 (2015) 124–137.
[53] V. Gabrel, C. Murat, A. Thiele, Recent advances in robust optimization: an overview, Eur. J. Oper. Res. 235 (3) (2014) 471–483.
[54] J.L. Hensen, R. Lamberts, Building Performance Simulation For Design and Operation, Routledge, 2012.
[55] S. Trzaska, E. Schnarr, A review of downscaling methods for climate change projections, in: African and Latin American Resilience to Climate Change (ARCC), United States Agency for International Development by Tetra Tech ARD, United States, 2014, pp. 1–42.
[56] A. Moazami, et al., Impacts of future weather data typology on building energy performance – Investigating long-term patterns of climate change and extreme weather conditions, Appl. Energy 238 (2019) 696–720.
[57] V.M. Nik, Making energy simulation easier for future climate – Synthesizing typical and extreme weather data sets out of regional climate models (RCMs), Appl. Energy 177 (2016) 204–226.
[58] V.M. Nik, Application of typical and extreme weather data sets in the hygrothermal simulation of building components for future climate – A case study for a wooden frame wall, Energy Build. 154 (2017) 30–45.
[59] Deru, M., et al., *US department of energy commercial reference building models of the national building stock*. 2011, National Renewable Energy Laboratory: 1617 Cole Boulevard Golden, Colorado.
[60] A.S. ASHRAE, Standard 90.1-2004, Energy standard For Buildings Except Low Rise Residential Buildings, American Society of Heating, Refrigerating and Air-Conditioning Engineers, Inc., 2004.
[61] M.A. Halverson, et al., ANSI/ASHRAE/IES Standard 90.1-2013 Determination of Energy Savings: Qualitative Analysis, Pacific Northwest National Laboratory (PNNL), United States, Washington, 2014.
[62] J. Zhang, et al., Energy and Energy Cost Savings Analysis of the IECC For Commercial Buildings, Pacific Northwest National Laboratory (PNNL), United States, Washington, 2013.

[63] ASHRAE, *Standard 169-2013, climate data for building design standards*," *1791 Tullie Circle NE• Atlanta, GA 30329*.
[64] D.B. Crawley, et al., EnergyPlus: creating a new-generation building energy simulation program, Energy Build. 33 (4) (2001) 319–331.
[65] US-DoE, Testing and Validation, EnergyPlus Energy Simulation Software, 2012 3/12/2012 [cited 2014 19/04/2014]; Available from:http://apps1.eere.energy.gov/buildings/energyplus/energyplus_testing.cfm.
[66] G.N. Walton, Thermal Analysis Research Program Reference Manual, National Bureau of Standards, United States, Washington, 1983.
[67] U. DoE, *EnergyPlus Input Output Reference*, US Department of Energy, 2010.
[68] SIA, *380/1*, Thermische Energie im Hochbau, 2009, Schweizerischer Ingenieur und Architektenverein, Zürich, 2009.
[69] Esteco, S.*ModeFRONTIER 2014 User's Manual*. 2014.
[70] K. Deb, et al., A fast elitist non-dominated sorting genetic algorithm for multi-objective optimization: nsga-ii, International conference on parallel problem solving from nature, Springer, 2000.
[71] E. Rigoni, S. Poles, NBI and MOGA-II, two complementary algorithms for multi-objective optimizations, in: Dagstuhl Seminar Proceedings, Schloss Dagstuhl-Leibniz-Zentrum für Informatik, 2005.
[72] C.M. Fonseca, P.J. Fleming, *Genetic algorithms for multiobjective optimization: formulationDiscussion and generalization*, Icga, 1993.
[73] O.B. Augusto, F. Bennis, S. Caro, A new method for decision making in multi-objective optimization problems, Pesqui. Operacional 32 (2012) 331–369.
[74] M. Hamdy, A.-.T. Nguyen, J.L.M. Hensen, A performance comparison of multi--objective optimization algorithms for solving nearly-zero-energy-building design problems, Energy Build. 121 (2016) 57–71.
[75] G.M. Mauro, et al., A new methodology for investigating the cost-optimality of energy retrofitting a building category, Energy Build. 107 (2015) 456–478.
[76] L. Ricco, E. Rigoni, Technical Report 2011-008, Esteco, 2011.
[77] C. Gu, Smoothing Spline ANOVA Models, 297, Springer Science & Business Media, 2013.